Electron and hole mobilities in semimetallic bismuth nanowires

Kiyoung Lee,[1] Seunghyun Lee,[2] S. N. Holmes,[3,*,†] Jinhee Ham,[2] Wooyoung Lee,[2,*,‡] and C. H. W. Barnes[1]
[1]*Department of Physics, Cavendish Laboratory, University of Cambridge, JJ Thomson Avenue, Cambridge CB3 0HE, United Kingdom*
[2]*Department of Materials Science and Engineering, Yonsei University, 134 Shinchon, Seoul 120-749, Republic of Korea*
[3]*Toshiba Research Europe Ltd., Cambridge Research Laboratory, 208 Cambridge Science Park, Milton Road, Cambridge CB4 0GZ, United Kingdom*

(Received 31 March 2010; revised manuscript received 28 October 2010; published 9 December 2010)

The Shubnikov de Haas effect is used to determine the electron and hole mobilities in a bismuth nanowire. We identify an excess hole density from a doping effect introduced during the on-film-formation-of-nanowires fabrication process. Three electron subbands and a single hole band contribute to the oscillatory magnetoresistance and these bands can be decomposed by fast Fourier transform analysis of ρ_{xx} into different orbits on an anisotropic Fermi surface. A nonharmonic Shubnikov de Haas oscillation from the hole band is due to variation in the carrier density with applied magnetic field. Electron and hole scattering is dominated by a short-range potential with a hole mobility of 5000 $cm^2\ V^{-1}\ s^{-1}$ and an electron mobility of 20 000 $cm^2\ V^{-1}\ s^{-1}$ at 1.6 K. Mobility analysis of the fast Fourier transform of ρ_{xx} is used to determine the individual three electron and single hole subband mobilities.

DOI: 10.1103/PhysRevB.82.245310 PACS number(s): 71.18.+y, 73.63.Nm, 81.07.Gf

I. INTRODUCTION

Nanowire growth technology has now reached the stage where many different metal, semimetal, and semiconductor systems can be fabricated in a conventional ultrahigh vacuum growth chamber using metal seed catalysts. Recent reviews[1,2] have outlined the potential for nanowires, with surround-gate channels and lateral *p-n* junctions or heterostructures being some of the exciting prospects. Nanowires are envisaged as potential channel replacement materials in complementary metal-oxide semiconductor (CMOS)-compatible logic device architectures and as device interconnects, if the challenges presented by control of the nanowire length, diameter, crystal orientation, and location can be overcome.[3]

Bismuth has a long history in condensed-matter physics due to the relatively easy ability to fabricate high-purity single crystals and the corresponding magnetotransport properties arising from a highly anisotropic Fermi surface.[4–6] The intrinsic semimetallic band structure has led to the observation of a semimetal-semiconductor transition[7] in thin film Bi, when the thickness (t) $<28\pm4$ nm. A similar transition in the Bi nanowire is predicted[8] to occur in the region of diameters (D) $<47\pm4$ nm. Bi-based devices have led on to topological insulators[9] and spintronic applications[10] where electrical spin injection and detection has been observed in a lateral spin-valve device at the level of 0.8% interfacial spin polarization. Bi nanowires also offer improvements in thermoelectric properties compared to bulk material.[8,11] Superconductivity has also been observed[12] in a 72 nm diameter Bi nanowire with a clear Shubnikov de Haas effect below the superconducting transition temperature. In fact both granular Bi nanowires[13,14] and single-crystal nanowires[15] fabricated by electrodeposition into porous polycarbonate membranes show clear effects of the transition to a superconducting state.

The Fermi surface of bulk Bi is composed of a single hole pocket at the T point (along the trigonal axis) and three electron pockets at the L points, slightly tilted to the binary-bisectrix plane. The electron-hole band overlap in the bulk is ~-40 meV. The Bi nanowires investigated here have been grown in a self-organized, Au-catalyst-free way from an initially sputtered polycrystalline Bi film. This has been termed the on-film-formation-of-nanowires (OFF-ONs) technique.[16] Previous structural and electrical measurements on OFF-ON devices have already demonstrated the high crystal quality compared to sputtered thin films, and confirmed that the growth direction is usually that of the (bulk) trigonal direction.[16,17] In fact the OFF-ON growth technique is extremely versatile and two crystal growth directions, [001] and also [110] can be stabilized. The nanowires can be switched from predominantly *n* type to predominantly *p* type by a backgate. A temperature-dependent magnetoresistance of 2500% (at 110 K in a field of 9 T) was observed[18] in previous OFF-ON Bi nanowires with an oscillatory Shubnikov de Haas effect only after an eighth-order polynomial was subtracted from R_{xx}.[17]

In the present work we quantify the Fermi-surface structure; the nanowires are *p* type possibly due to an unintentional acceptor level introduced during the growth process. The Fermi-surface properties have been quantified using the anisotropy in the Shubnikov de Haas effect for different magnetic field orientations with respect to the nanowire axes.[4] The electron and hole mobilities are determined from a mobility analysis[19] of the fast Fourier transform (FFT) of R_{xx}.

II. DEVICE PREPARATION

The Bi nanowire measured in this work is 120 μm long and has a diameter of 400 nm. Previous measurements[16] have identified the outer amorphous oxide (Bi_2O_3) thickness as 10 nm, so in this case the electrical diameter is reduced to 380 nm. Figure 1(a) shows a scanning electron microscope (SEM) image of the nanowire that was measured. The nanowires are placed randomly on the SiO_2-Si substrate and four

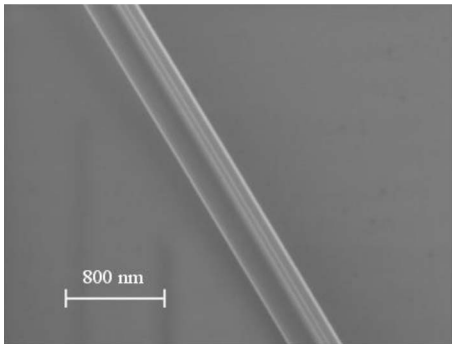

(a)

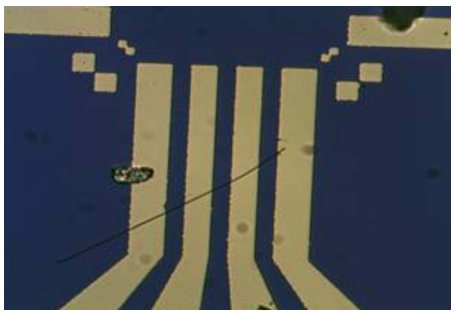

(b)

FIG. 1. (Color online) (a) An SEM image of a single Bi nanowire. The physical diameter is approximately 400 nm and length 120 μm. (b) An optical image of the 400 nm diameter device showing the current and voltage probes.

Ti-Au electrical contacts are deposited using optical lithography, see Fig. 1(b). The ohmic electrical contacts are made by removing the Bi_2O_3 prior to deposition with an Ar-ion sputtering technique.[16] The contact resistance varied between devices from 700 to 2300 Ω per contact in an area of 6 μm^2 corresponding to resistance-area product in the range 4–14 kΩ μm^2.

Magnetic fields up to 10 T (at 350 mK to 1.7 K) could be applied parallel to the wire in plane (the trigonal direction) or perpendicular to the wire (in the bisectrix-binary plane). Two perpendicular directions were accessible, either perpendicular to the Si substrate or perpendicular to the wire but in the plane of the substrate. Quasi-dc currents of 10–150 nA were used and excitation voltages were kept $< \frac{k_B T}{e}$, where T is the measurement temperature, to prevent carrier heating effects that reduce the amplitude of the Shubnikov de Haas oscillations. The transport is in the diffusive regime in the present devices, although we show that the electron mean-free path (λ) is $\sim \frac{1}{2}D$. With a 380 nm wire diameter, one-dimensional (1D) behavior is possibly weak, in fact the magnetic length $l_B = \sqrt{\hbar/eB}$ is <190 nm in an applied magnetic field (B) of ~ 0.02 T and the Shubnikov de Haas effect in R_{xx} at significantly higher fields should be mostly representative of bulk bismuth.

Figure 2 shows the temperature-dependent resistance ratio where the resistance at 300 K is 1.0 kΩ. This increase in resistance below 300 K is typical behavior for an extrinsic semimetal or a narrow band-gap semiconductor. The decrease in resistance below 30 K could be due to an increase in mobility. The dashed line shows the resistance ratio in an applied magnetic field of 0.25 T applied parallel to the long axis of the wire. This curve should be more representative of the bulk Bi crystal as $l_B < \frac{1}{2}D$. Weak localization or antiweak localization effects are small in these nanowires.

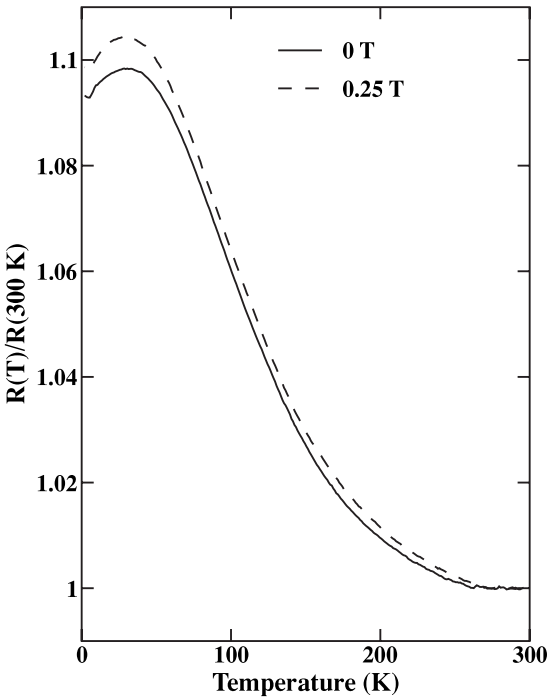

FIG. 2. The resistance ratio as a function of temperature in zero applied field and magnetic field of 0.25 T applied along the wire.

III. FERMI-SURFACE DETERMINATION

In the geometry of applied magnetic field perpendicular to the substrate, three series of Shubnikov de Haas oscillations can be observed in R_{xx}. These correspond to the three electron ellipsoidal bands at the L points with similar mobility (μ_n) but different carrier density. Figure 3 shows the oscillatory structure in R_{xx} at 356 mK after subtracting a background *linear* variation of 431 $\Omega\,T^{-1}$ in this orientation. This enhances the oscillatory structure although an FFT is used to determine the fundamental field (B_f) of the component oscillations (in dR_{xx}/dB). The carrier density (n or p) can then be *estimated* from the Landau-level degeneracy in a three-dimensional electron gas using Eq. (1),

$$n = \frac{1}{3\pi^2}\left(\frac{2e}{\hbar}\right)^{3/2} B_f^{3/2} \quad \text{(valid for } n \text{ or } p\text{)}. \tag{1}$$

This is strictly valid for a spherical Fermi surface. Corrections due to an ellipsoidal Fermi surface include the term $(B_{f\perp}B_{f\parallel}^2)^{1/2}$ rather than $B_f^{3/2}$, where $B_{f\perp}$ is the fundamental field perpendicular to the major axis of the ellipsoid and $B_{f\parallel}^2$ is the fundamental field parallel to the major axis of the ellipsoid. Confinement tends to modify the ellipsoidal structure in Bi resulting in a more spherical Fermi surface.[20]

The inset of Fig. 3 shows the FFT of the oscillatory R_{xx} in the field domain 0.2–3.9 T. The three peaks in the FFT (e1, e2, and e3) have similar width and this is confirmation that it

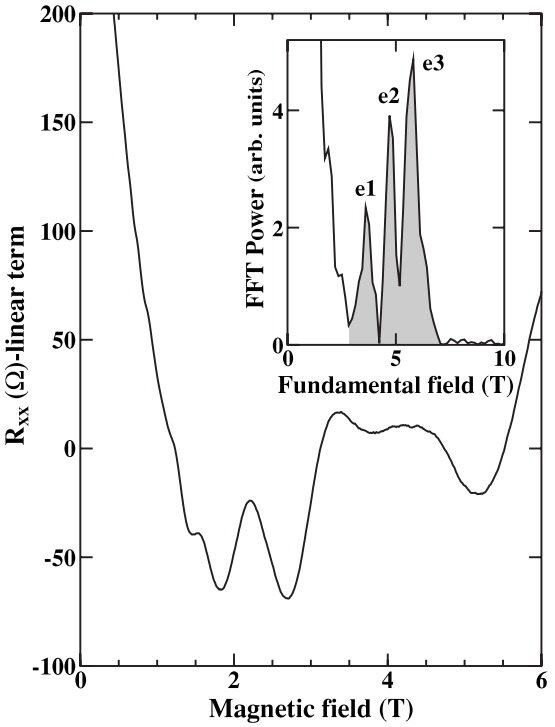

FIG. 3. R_{xx} (minus a linear term) at 356 mK in perpendicular field to 6 T, the inset shows the three electron subbands in the FFT. The FFT was taken in the magnetic field domain 0.2–3.9 T.

is three electron bands that are observed in this geometry. The frequency response in the FFT at $B_f < 2$ T is the result of the large magnetoresistance background in R_{xx}. A hole Shubnikov de Haas effect is suppressed with the applied field along the bisectrix-binary directions of the Fermi surface. The magnetoconductivity (σ_{xx}) was also measured in a two-contact geometry, however the oscillatory structure in σ_{xx} is not as clear as that in R_{xx} due to the contributions of a high contact resistance.

Magnetic field modulation was also used in this work at 1.7 K, see Fig. 4 which shows oscillatory structure in the analog dR_{xx}/dB signal down to 0.5 T. The shaded region shows $\mu_n \cdot B < 1$ with $\mu_n \sim 20\,000$ cm^2 V^{-1} s^{-1} in this case and the reproducibility in the oscillatory structure between two different sweeps is shown. This technique is a more sensitive method of measuring dR_{xx}/dB compared to numerical differentiation of R_{xx} and follows a method described previously.[21] A sinusoidal 6.6 mT field is applied at $\omega = 33.3$ Hz and the oscillatory signal in R_{xx} at frequency ω has an amplitude proportional to dR_{xx}/dB. In Fig. 4 it appears that dR_{xx}/dB has a negative gradient but this is a systematic error in setting the phase of the oscillation due to induced nonoscillatory voltages in the measuring circuit at frequency ω. No complications due to spin splitting of the electron bands are observed (up to 3.9 T). This would be evident as second harmonics in the FFT spectrum of R_{xx}, these are absent in the inset of Fig. 3. Magnetic field modulation was used in all applied magnetic field geometries although it is particularly advantageous when there is a large nonoscillatory background signal.

With the applied magnetic field in plane and along the wire axis (the trigonal bulk Fermi-surface direction) a hole

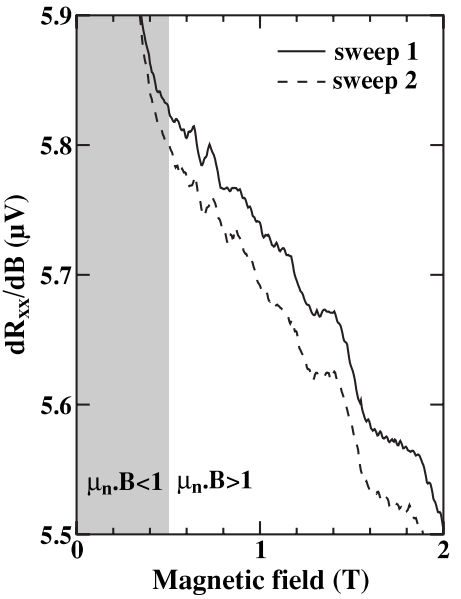

FIG. 4. The analog dR_{xx}/dB signal from magnetic field modulation at 1.7 K up to 2 T. The y-axis scale is measured in microvolt with a dc source-drain current of 150 nA and a modulated magnetic field of 6.6 mT. The shaded region corresponds to that where $\mu_n \cdot B < 1$.

Shubnikov de Haas effect dominates R_{xx}. This is characterized by the oscillatory structure in R_{xx} starting at much higher applied field, 2 T in this case, see Fig. 5. This is coming from a single band of holes and the oscillatory structure is nonharmonic at low filling factors. Consequently an FFT of the data is distorted somewhat and as the structure in R_{xx} is coming from a single subband then simple harmonic

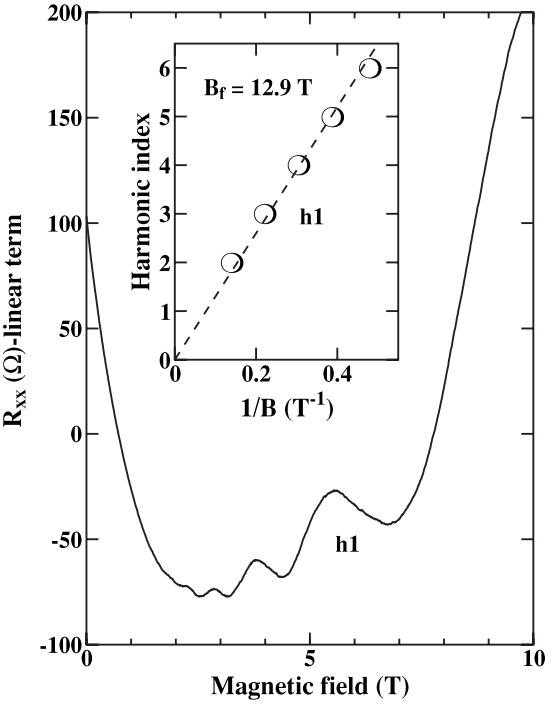

FIG. 5. R_{xx} (minus a linear term) at 700 mK in parallel field, the inset shows a harmonic R_{xx} minima plot against $1/B$.

TABLE I. A summary of the Shubnikov de Haas effect frequency components in different magnetic field orientations.

Field orientation	B_f (T)	Δ (T^{-1})	Carrier type	Band	Estimated density (cm^{-3})
B perpendicular to Si substrate (bisectrix-binary)	3.63	0.275	*n*	e1	3.9×10^{16}
	4.65	0.215	*n*	e2	5.7×10^{16}
	5.63	0.178	*n*	e3	7.6×10^{16}
					1.7×10^{17}
B parallel to wire (trigonal)	12.9	0.078	*p*	h1	2.6×10^{17}
B perpendicular to wire (bisectrix-binary)	10.7	0.093	*p*	h1	2.0×10^{17}
	3–5.5[a]		*n*	e1-e3[a]	

[a]The electron bands are unresolved in the FFT for this geometry.

number analysis can be used to determine the hole density. A harmonic number analysis based on Eq. (2) can be used to determine the fundamental field,

$$N \cdot B_N = B_f = \frac{1}{\Delta(1/B)}. \tag{2}$$

B_N is the magnetic field position of the Nth minimum in the oscillation in ρ_{xx}, N is an integer, and $\Delta(1/B)$ is the inverse field period. The fundamental oscillation where $N=1$ is at the fundamental field, however the quantum limit where a single spin-split Landau level is occupied, is at $2B_f$.

Figure 5 (inset) shows the harmonic analysis for the field applied in the direction parallel to the wire (trigonal direction). A small change in the hole density with field can account for the nonharmonic behavior of the fit in the Fig. 5 inset. This variation in hole density is characteristic of the onset of a semimetal-to-semiconductor transition.[7] The fundamental field of the hole band is 12.9 T and corresponds to a hole density of 2.6×10^{17} cm^{-3} (at higher filling factors). The inverse field period $\Delta(1/B)$, can be used to calculate the area of the Fermi surface perpendicular to the applied field $[A_{extremal}=\frac{2\pi e}{\hbar}\frac{1}{\Delta(1/B)}]$. The hole band is ellipsoidal with the trigonal direction corresponding to the smallest $A_{extremal}$ value. Rotating the applied field away from the trigonal direction increases $A_{extremal}$ and reduces Δ, the hole orbit can become "openlike" and disappears from the oscillatory R_{xx}. This anisotropic Fermi surface is bulklike and as the Fermi surface occupies $\sim10^{-5}$ of the Brillouin-zone boundary,[6] this reduces any possible extended-zone schemes that could give rise to oscillatory R_{xx} away from the trigonal direction. Table I is a summary of the Shubnikov de Haas frequency components of the bismuth nanowire for different magnetic field orientations. The estimated carrier densities and the number of electron and hole bands are similar to values in the literature for bulk, thin-film bismuth[22,23] although we have identified an excess hole density ($\Delta p\sim9\times10^{16}$ cm^{-3}) in these OFF-ON fabricated nanowires. No trigonal direction electron band(s) is (are) observed.

With the applied magnetic field perpendicular to the wire (in plane) R_{xx} shows both an electron and hole Shubnikov de Haas oscillation, see Fig. 6. The hole band is again nonharmonic but has a distinct power spectrum at higher filling factors. Figure 6 shows the oscillatory R_{xx} after a linear term, 380 Ω T^{-1} is subtracted in this orientation. There is a variation in hole density between different cooldowns and this could be due to *p*-type dopant activation differences although there is no persistent change in carrier density with broadband illumination at low temperatures.

The fundamental field is 10.7 T from Eq. (2). This agrees with the peak labeled as h1 in the FFT spectrum, see the inset of Fig. 6. In molecular-beam epitaxy (MBE) grown Bi films[7] the influence of a surface acceptor was identified producing a sheet hole density of 8×10^{12} cm^{-2} with a measured bulk density of $8\times10^{12}/t$ cm^{-3} with t in centimeter units. The three electron subbands are unresolved in the FFT spectrum in this particular bisectrix-binary geometry.

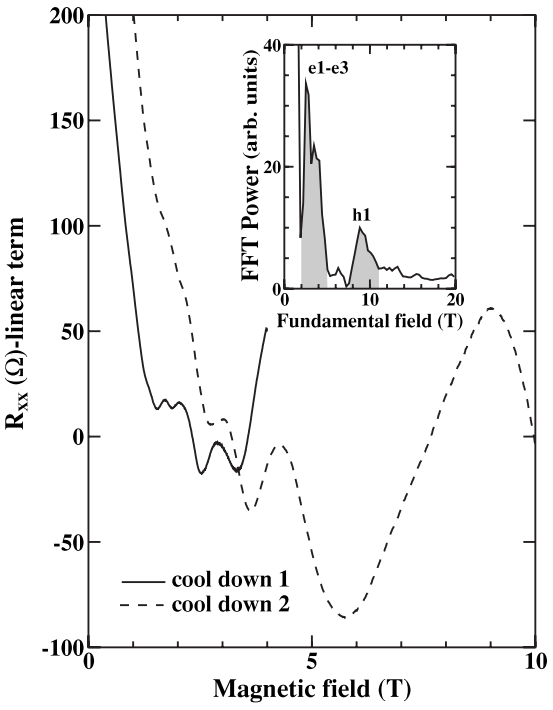

FIG. 6. R_{xx} (minus a linear term) at 1.7 K in the magnetic field perpendicular to the wire in plane, the inset shows an FFT with the three (unresolved) electron subbands and a nonharmonic hole band.

TABLE II. Analysis of the FFT peak widths for the individual electron and hole subbands.

FFT peak	δB, half width at half height of the FFT peak (T)	μ_q from Eq. (3)[a] ($cm^2\ V^{-1}\ s^{-1}$)
e1	0.28	21000
e2	0.26	23000
e3	0.28	21000
h1	1.11	5300

[a]Assuming a field damping term of $e^{-(2\pi/\mu_q B)}$ in the Shubnikov de Haas oscillation.

IV. MOBILITY SPECTRUM ANALYSIS

The half width of the FFT peak (δB) is related to the single particle or quantum mobility (μ_q),[19] see Eq. (3),

$$\mu_q = (4^{1/3} - 1) \cdot \frac{1}{\delta B}, \tag{3}$$

where δB is the half width at half height of the peak in the FFT power spectrum of dR_{xx}/dB. This mobility analysis is modified to $\mu_q = \sqrt{3} \cdot \frac{1}{\delta B}$ for the FFT power spectrum of the nondifferentiated R_{xx} data. This theory was originally derived for slab and δ-doped GaAs two-dimensional electron systems and in the quasi-three-dimensional electron gas in the nanowire, the magnetic field damping term for the Shubnikov de Haas oscillation is $e^{-(2\pi/\mu_q B)}$ rather than $e^{-(\pi/\mu_q B)}$ in a strictly two-dimensional system and Eq. (4) has been modified from the two-dimensional expression derived in Ref. 19. In the Bi nanowires the scattering is by a short-range potential and the quantum and transport mobilities are equal to a good approximation.

Table II shows an analysis of the FFT peak widths from the field perpendicular to the substrate geometry (the bisectrix-binary plane) and the field perpendicular to the wire (in plane). It is clear that the single-particle electron mobility is $>20\,000\ cm^2\ V^{-1}\ s^{-1}$ and single-particle hole mobility $>5000\ cm^2\ V^{-1}\ s^{-1}$. These values of mobility agree with the condition $\mu \cdot B > 1$ for the onset of the Shubnikov de Haas effect in R_{xx}. There are some minor corrections (these are discussed in Ref. 19) to the analysis of the FFT peak widths, particularly as the FFT data domain is typically 0.3–4 T rather then including fields up to the fundamental field of the hole Shubnikov de Haas effect ~12.9 T in the trigonal geometry. The minor corrections due to the finite data set have the effect of broadening the FFT peaks, however this effect is smaller than the experimental error.

We develop a similar theme for the peak heights in the FFT power spectrum. The peak heights[19] in the FFT are proportional to $n\mu_n^2$ for the electron gas and $p\mu_p^2$ for the hole gas. The relative electron-to-hole peak height, $(n\mu_n^2/p\mu_p^2)$ should be ~3.5 according to the values for n (the e2 band) $=5.7\times10^{16}\ cm^{-3}$, $p=2.6\times10^{17}\ cm^{-3}$, $\mu_p = 5000\ cm^2\ V^{-1}\ s^{-1}$, and $\mu_n = 20\,000\ cm^2\ V^{-1}\ s^{-1}$. From the inset of Fig. 6 the peak height ratio in the FFT is 3.3 confirming the electron and hole mobility values and the FFT peak assignment to separate electron and hole contributions.

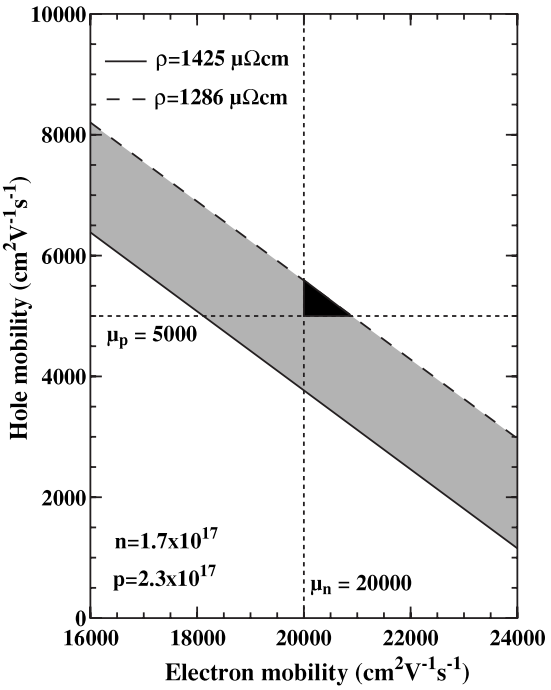

FIG. 7. Contours of constant resistivity for variations in electron and hole mobility. The shaded area is the region of possible multiband fits at 1.6 K. The dotted lines correspond to the electron and hole mobilities determined from the onset of the Shubnikov de Haas effects. The dark area corresponds to the most likely mobilities.

The resistance of the nanowire is 1.1 kΩ at 1.6 K and the resistivity (ρ) is given by $\rho = \frac{\pi D^2 R}{4L_v}$ in a cylinder of diameter D, where R is the resistance between the voltage contacts L_v apart. This gives 1286 $\mu\Omega$ cm (380 nm diameter) or 1425 $\mu\Omega$ cm for 400 nm ignoring the effects of the Bi_2O_3 outer layer. A multicarrier fit to ρ in zero applied magnetic field, where $\frac{1}{\rho} = ne\mu_n + pe\mu_p$ was then used to determine the electron mobility and the hole mobility with the measured electron and hole carrier densities estimated from the Shubnikov de Haas effect. This is strictly valid only at $B=0$ and in small finite fields (where $\mu_n \cdot B < 1$ and $\mu_p \cdot B < 1$) a multicarrier fit will be complicated by 1D behavior and the fact that the Hall constant cannot be measured or the coupled Hall constant equation solved in a nanowire. Figure 7 shows a contour plot of constant resistivity (with and without Bi_2O_3) for possible electron and hole mobilities with the measured n and p values. The light-shaded areas are possible values of μ_n and μ_p from the multicarrier fit. The single-particle mobility values ($20\,000\ cm^2\ V^{-1}\ s^{-1}$ for electrons and $5000\ cm^2\ V^{-1}\ s^{-1}$ for holes) are the dotted lines and represent the lower limits to the transport mobilities; this reduces the range in solutions of the multicarrier fit to the dark-shaded area with $\mu_p = 5300 \pm 300\ cm^2\ V^{-1}\ s^{-1}$ and $\mu_n = 20\,500 \pm 500\ cm^2\ V^{-1}\ s^{-1}$. The hole mobility is comparable to that observed in MBE-grown bulk Bi films for thicknesses ~40 nm but below that in 500-nm-thick films[7] whereas the electron mobility is higher than a 500-nm-thick film. The mean-free path (λ) in Bi is known to be extremely long in bulk crystals.[5] Here we calculate λ assuming that the Fermi surface can be described by an average wave number

$\langle k_f \rangle$, where $\lambda = \frac{\hbar \langle k_f \rangle \mu}{e}$. According to the measured carrier concentrations summarized in Table I, $\langle k_f \rangle$ is 1.7×10^8 m^{-1} for electrons and 2.0×10^8 m^{-1} for holes. This gives values for the mean-free path of 240 nm for electrons and 70 nm for holes in a 380 nm diameter Bi nanowire.

V. SUMMARY

The bismuth nanowire mobilities are high enough to observe clear Shubnikov de Haas oscillations in R_{xx}. There are no quantifiable 1D effects such as quantized conductance at a diameter of 380 nm. We have used a mobility analysis of the FFT spectrum of R_{xx} to identify individual electron and hole subband mobilities and have estimated the carrier densities from the resolvable fundamental field values. The electron mean-free path is $\sim \frac{1}{2}D$ so minor improvements in the OFF-ON crystal growth method will ensure that the ballistic transport regime can be studied for electrons, however hole transport will still be diffusive in the nanowires. This should not hinder future quantum transport measurements in narrower Bi nanowires as they are predicted[8] to be semiconducting below ~50 nm diameter where the trigonal hole band is nonconducting (fully occupied by electrons).

A possible excess hole density in the nanowire could be due to an unintentional *p*-type doping in the growth process rather than an intrinsic or band-structure modification effect. If this excess hole density is coming from a surface acceptor state then the excess hole density should vary as $\sim 1/D$ for unity activation of the acceptor and this can be verified once smaller diameter nanowires are available. On the plus side, a resistivity of ~1000 $\mu\Omega$ cm coupled with an Au-free fabrication process are parameters required for CMOS channel replacement according to the 2007 ITRS. The well-defined Fermi surface quantified here is due to the high-quality single-crystal Bi nanowire where the mobilities are comparable to MBE-grown Bi and are significantly higher than those in the starting films of sputtered Bi.

ACKNOWLEDGMENTS

This work has equal contributions from the authors K.L. and S.L. W.L. acknowledges the support of Priority Research Centers Program (Grant No. 2009-0093823) through the National Research Foundation of Korea (NRF) and the "Center for Nanostructured Materials Technology," under the "21st Century Frontier R&D Programs" of the Ministry of Education, Science and Technology.

*Corresponding author.
†s.holmes@crl.toshiba.co.uk
‡wooyoung@yonsei.ac.kr

[1] C. Jagadish, Semicond. Sci. Technol. **25**, 020301 (2010).
[2] W. Lu and C. M. Lieber, J. Phys. D: Appl. Phys. **39**, R387 (2006).
[3] http://www.itrs.nest/Links/2007ITRS/Home2007.htm
[4] D. Shoenberg, Proc. R. Soc. London, Ser. A **170**, 341 (1939).
[5] A. B. Pippard and R. Chambers, Proc. Phys. Soc., London, Sect. A **65**, 955 (1952).
[6] V. Édel'man, Adv. Phys. **25**, 555 (1976).
[7] C. A. Hoffman, J. R. Meyer, F. J. Bartoli, A. Di Venere, X. J. Yi, C. L. Hou, H. C. Wang, J. B. Ketterson, and G. K. Wong, Phys. Rev. B **48**, 11431 (1993).
[8] Y.-M. Lin, X. Sun, and M. S. Dresselhaus, Phys. Rev. B **62**, 4610 (2000).
[9] H. Peng, K. Lai, D. Kong, S. Meister, Y. Chen, X.-L. Qi, S.-C. Zhang, Z.-X. Shen, and Y. Cui, Nature Mater. **9**, 225 (2010).
[10] K.-I. Lee, J. W. Roh, J. Chang, S.-H. Han, K.-H. Shin, W. Y. Jeung, M. Johnson, and W. Lee, Phys. Rev. B **79**, 195201 (2009).
[11] J. Heremans and C. M. Thrush, Phys. Rev. B **59**, 12579 (1999).
[12] M. Tian, J. Wang, Q. Zhang, N. Kumar, T. E. Mallouk, and M. H. W. Chan, Nano Lett. **9**, 3196 (2009).
[13] M. Tian, J. Wang, N. Kumar, T. Han, Y. Kobayashi, Y. Liu, T. E. Mallouk, and M. H. W. Chan, Nano Lett. **6**, 2773 (2006).
[14] M. Tian, N. Kumar, M. H. W. Chan, and T. E. Mallouk, Phys. Rev. B **78**, 045417 (2008).
[15] Z. Ye, H. Zhang, H. Liu, W. Wu, and Z. Luo, Nanotechnology **19**, 085709 (2008).
[16] Wooyoung Shim, Jinhee Ham, Kyoung-Il Li, Won Yong Jeung, Mark Johnson, and Wooyoung Lee, Nano Lett. **9**, 18 (2009).
[17] W. Shim, J. Ham, J. Kim, and W. Lee, Appl. Phys. Lett. **95**, 232107 (2009).
[18] W. Shim, D. Kim, K.-I. Li, S.-H. Han, W. Y. Jeung, M. Johnson, and W. Lee, J. Appl. Phys. **104**, 073715 (2008).
[19] E. Skuras, R. Kumar, R. L. Williams, R. A. Stradling, J. E. Dmochowski, E. A. Johnson, A. Mackinnon, J. J. Harris, R. B. Beall, C. Skierbeszewski, J. Singleton, P. J. van der Wel, and P. Wisiewski, Semicond. Sci. Technol. **6**, 535 (1991).
[20] T. E. Huber, K. Celestine, and M. J. Graf, Phys. Rev. B **67**, 245317 (2003).
[21] D. Shoenberg, *Magnetic Oscillations in Metals* (Cambridge University Press, Cambridge, England, 1984).
[22] D. L. Partin, J. Heremans, D. T. Morelli, C. M. Thrush, C. H. Olk, and T. A. Perry, Phys. Rev. B **38**, 3818 (1988).
[23] F. Y. Yang, Kim Liu, Kimin Hong, D. H. Reich, P. C. Searson, C. L. Chien, Y. Leprince-Wang, K. Yu-Zhang, and Ke Han, Phys. Rev. B **61**, 6631 (2000).